
Vision-centric Token Compression in Large Language Model

Ling Xing^{1*}, Alex Jinpeng Wang^{2*}, Rui Yan^{1†}, Xiangbo Shu¹, Jinhui Tang³

¹Nanjing University of Science and Technology ²Central South University

³Nanjing Forestry University

Abstract

Real-world applications are stretching context windows to hundreds of thousand of tokens while Large Language Models (LLMs) swell from billions to trillions of parameters. This dual expansion send compute and memory costs skyrocketing, making *token compression* indispensable. We introduce VISION CENTRIC TOKEN COMPRESSION (VIST), a *slow–fast* compression framework that mirrors human reading: the *fast* path renders distant tokens into images, letting a **frozen, lightweight vision encoder** skim the low-salience context; the *slow* path feeds the proximal window into the LLM for fine-grained reasoning. A Probability-informed Visual Enhancement (PVE) objective masks high-frequency tokens during training, steering the Resampler to concentrate on semantically rich regions—just as skilled reader gloss over function words. On eleven in-context learning benchmarks, VIST achieves the same accuracy with $2.3 \times$ fewer tokens, cutting FLOPs by 16% and memory by 50%. This method delivers remarkable results, outperforming the strongest text encoder-based compression method CEPE by **7.6%** on average over benchmarks like TriviaQA, NQ, PopQA, NLUI, and CLIN, setting a new standard for token efficiency in LLMs. The project is at <https://github.com/CSU-JPG/VIST>.

1 Introduction

Large language models (LLMs) excel at short snippets, yet many real-world tasks, *e.g.*, long-document understanding [1, 2] and question answering [3, 4]—already require inputs far beyond the thousand-token regimes of early GPT-3 [1]. At the same time, parameter counts have leapt from billions to trillions [5, 6, 7]. In this dual squeeze of *longer context & larger models*, **compression shifts from a convenience to a necessity**: without shrinking the input, even the most powerful LLM cannot afford to reason over the information we want it to see.

Psycholinguistics shows that our eyes dance across text: we *fixate* on rare, content-rich words and *skip* almost one-third of high-frequency function words [8, 9, 10]. This *selective-reading* strategy forms a natural *slow–fast* circuit. A *fast visual pass* skims distant, low-salience context to maintain global context, while a *slow cognitive pass* focuses on nearby sentences that matter. (Figure 1 (a)).

Motivated by this circuit, we present VISION CENTRIC TOKEN COMPRESSION (**VIST**), a *slow–fast* token compression framework that mirrors human skimming. As illustrated in Figure 1 (b), VIST first converts loosely relevant long context into images, which are processed by a frozen vision encoder and a trainable Resampler to produce semantically compact visual tokens. These compressed tokens and the main input tokens are then consumed by the LLM. In this *slow–fast* setup, the *vision encoder*

* Equal contribution

† Corresponding author

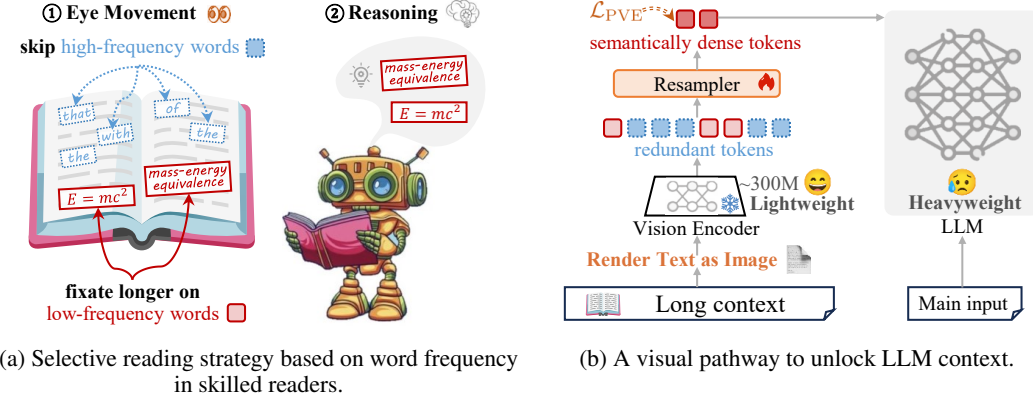


Figure 1: Our method **VIST** adopts a lightweight vision encoder to process loosely relevant long contexts, offering a **more cost-efficient alternative** to full LLM processing. However, the inherent redundancy in long text leads to redundant visual tokens. Motivated by **Selective Reading Strategy** where *low-frequency (content) words receive longer fixations while high-frequency function words are often skipped*, we design Probability-informed Visual Enhancement (*i.e.*, \mathcal{L}_{PVE}). This guides the Resampler to prioritize informative content over redundancy, **resulting in a 75% reduction in the number of visual tokens** and yielding semantically dense tokens.

acts like the human eye—selectively attending to salient information—while the LLM functions as the brain, concentrating on the most informative content for deeper reasoning.

Specifically, the frozen visual encoders (*e.g.*, CLIP [11]) trained on paired image-text data naturally *acquire OCR capabilities* [11, 12], making them a powerful tool for image-based text understanding. However, the inherent redundancy in long text leads to redundant visual tokens. To address the problem, we design **Probability-informed Visual Enhancement** (PVE), a contrastive scheme that enforces Resampler to prioritize informative content over redundancy. Concretely, PVE applies **frequency-based masking strategy** to text token embeddings from the LLM tokenizer, suppressing high-frequency (less informative) text tokens. This semantically rich text supervision guides the Resampler to focus on informative content, bridging the semantic gap between visual and text tokens, and enabling more effective token compression. Unlike previous work [13, 14, 15, 16, 17] that rely on LLMs to compute token-level information entropy for assessing importance, VIST adopts token frequency as a simple yet effective proxy, and further **reveals rare tokens are key contributors to overall semantic meaning** (*cf.* Figure 3 and §5).

VIST leverages a lightweight vision encoder to compress loosely relevant long contexts, offering a cost-efficient alternative to full-scale LLM computation. Furthermore, the vision encoder serves as a *visual text tokenizer*, offering several compelling advantages over traditional text tokenizers. **1 Simplified Tokenization.** Text tokenizers rely on complex tokenization rules and vocabulary constraints, typically involving nearly ten human-defined preprocessing steps (*e.g.*, lowercasing, punctuation and stop word removal, and tokenization) [18]. However, the vision encoder processes text more directly by treating rendered text images as visual inputs. **2 Vocabulary Bottleneck Mitigation.** Text tokenization, constrained by a finite vocabulary, becomes a bottleneck when scaling to many languages. A larger vocabulary increases memory and computational costs in the embedding matrix and output layer. However, vision encoder eliminates the need for text tokenizers and unifies various languages into a single image format that removes the need for a vocabulary [19, 20]. **3 Robustness to Character-Level Noise.** Vision encoders are more resilient to typos and low-level orthographic attacks, as they capture holistic visual patterns rather than relying on discrete token matching [20]. **4 Multilingual Efficiency.** While our work focuses on English, visual text tokenizer can reduce the number of tokens compared to traditional text tokenizer for languages (*e.g.*, 62% for Japanese, 78% for Korean, and 27% for Chinese). This reduction is particularly impactful in long-text scenarios. Taken together, *leveraging vision encoders for long-context compression is a promising and worthwhile direction to explore*.

To validate the effectiveness of VIST, we primarily compare with the text-encoder-based token compression counterpart CEPE [21]. VIST requires **2.3 \times fewer visual tokens** than text tokens for the same input, reducing **FLOPs by 16%** and **memory usage by 50%**. VIST also delivers consistent

gains over CEPE on both In-Context Learning and Open-domain Question Answering tasks, with **average gains of 3.6% across 11 datasets** and **5.7% across 3 datasets**, respectively—highlighting the effectiveness of visual representations for long-context modeling in LLMs.

2 Related Work

Token Compression. There has been a growing interest in expanding the context window for LLMs. A line of methods leverages LLM itself to compress raw long input. One may classify these works into two principal groups. **i)** *soft prompt-based* methods that adapt LLMs to compress context into fewer tokens [22, 23, 24, 25, 26]. **ii)** *selection-based* methods that remove redundant tokens based on information entropy computed by LLMs [13, 14, 15, 16, 17, 27]. All the long inputs typically need to be handled by the heavy LLMs, which incur high costs. Another line of work [28, 29] augments LLMs with the capacity to memorize previous long context information by external memory bank and retrieve relevant knowledge [30, 31, 32, 33]. Our method is orthogonal to these existing strategies and can be combined with them to achieve longer context length. The most related work is CEPE [21], which employs a lightweight text encoder to handle long contexts and integrates the information into LLM via cross-attention. While CEPE reduces workload on the LLM, it overlooks the redundancy in long text, making it harder for LLMs to effectively allocate attention to key content. In contrast, VIST compresses long text into compact visual tokens guided by high-density semantic text tokens.

Vision-centric Method. Text tokenization [34, 35, 36] breaks down text into tokens, serving as a fundamental step in natural language processing. However, tokenization-based methods lack robustness against spelling errors and face vocabulary bottlenecks. A new line of work tackles these issues in a tokenizer-free paradigm [37, 20, 38]. The representative method Pixel [20] renders text as images and learns to reconstruct masked image patches at the pixel level. It demonstrates strong cross-language translation capabilities and tolerance for text perturbation. Along this direction, recent work explores different pre-training objectives [39, 40], *e.g.*, contrastive learning [41], patch-and-text prediction [38]. Despite advancements, these methods overlook long-text scenarios and rely on complicated training pipelines, *e.g.*, OCR-based text understanding [19]. In contrast, VIST directly processes text images by leveraging a vision encoder pretrained on image-text pairs with strong OCR capabilities, and enhancing visual features using enriched text embeddings from LLM tokenizer. An emerging family of multimodal methods [42, 43, 44, 45, 46] leverage visual representations to process text and images together, enabling a wide range of applications involving visually-situated text, *e.g.*, webpage parsing [43], tables images analysis [47], and document understanding [42, 48]. In this work, we explore incorporating long-context information into LLMs from a visual perspective.

3 Methodology

In this section, we present our method VIST, which processes long in-context text by a lightweight visual encoder, effectively and efficiently extending the context length of LLMs.

3.1 Overall Pipeline

Our VIST, a *slow-fast* compression framework, is designed to efficiently process long texts by mimicking human reading. The *fast visual path* skims distant, low-salience long context via a lightweight vision encoder, while the *slow cognitive path* performs fine-grained reasoning on important content by LLM. As illustrated in Figure 2, the input long text (*i.e.*, T text tokens) is split into two parts: the first T_e text tokens processed in a visual view and the remaining T_d raw text tokens given to LLM, where $T = T_e + T_d$. Specifically, the T_e text tokens are evenly rendered into M images and fed into a frozen vision encoder. Then VIST employs a learnable Perceiver Resampler to compress text-rendered image features into a fixed count of tokens. Such compressed visual tokens are integrated into the LLM via cross-attention for the next-token prediction. The Perceiver Resampler is jointly trained with the LLM during tuning the cross-attentions in an end-to-end manner.

To empower the model with the ability to comprehend dense text in images, we devise **Probability-informed Visual Enhancement** (PVE, §3.4). PVE maximizes agreement between visual features obtained from the Perceiver Resampler and **text token embeddings extracted from LLM tokenizer**. This alignment bridges the global semantic gap between visual tokens and raw text tokens. Furthermore, to address token redundancy, VIST incorporates a **frequency-based masking** mechanism

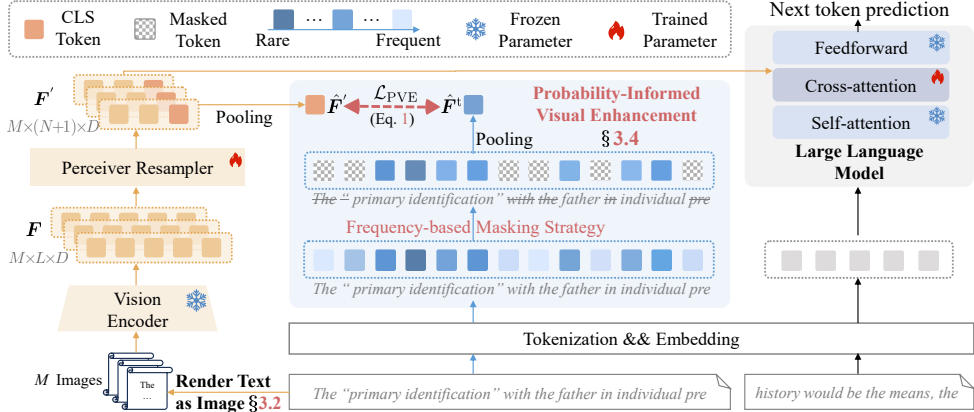


Figure 2: **Overview of VIST.** VIST, a *slow-fast* token compression framework, efficiently processes long texts by mimicking human skimming. First, the *fast visual path* converts long context into images and employs a lightweight vision encoder to capture semantically compact visual features. These features are then integrated into the LLM via cross-attention in the *slow cognitive path*, allowing LLM to focus on salient content for deeper reasoning. To prioritize informative content in text images, VIST employs **Frequency-based Masking** on text token embeddings from text tokenizer, suppressing high-frequency but low-information token (e.g., “the” and “with”). Such refined embeddings guide the Resampler in extracting critical semantics from the images.

within PVE that selectively masks high-frequency, low-information text tokens, thereby improving the information density of the text embeddings. These refined embeddings serve as enriched supervision signals, encouraging visual features to be more compact and semantically meaningful.

3.2 Vision-centric Implementation

VIST transforms raw textual data into M uniformly distributed RGB images $\mathcal{X} = \{x_m \in \mathbb{R}^{H \times W \times C}\}_{m=1}^M$, where M can be dynamically adjusted based on the length of the input text. Concretely, each image is configured with height $H = 14$, width $W = 3,584$, and $C = 3$ RGB channels, which corresponds to a square color image with a resolution of 224×224 . Text is rendered using a 10px font size and Google *Noto Sans* typeface. If text incompletely fill the image, white empty patches are masked to exclude them from attention score computation and loss calculation. Compared to text tokenizer-based methods, this rendering method does not lead to slower training speeds [44].

3.3 Token Reduction

The M text-rendered images are first processed by frozen vision encoder, specifically the ViT-L/14 [11] from OpenCLIP. The extracted features $F \in \mathbb{R}^{M \times L \times D}$ are then fed into a trainable Perceiver Resampler [49], producing a fixed set of $N+1$ visual tokens per image (including a CLS token), denoted as $F' \in \mathbb{R}^{M \times (N+1) \times D}$, where $N = 64$ and D is the feature dimension. During training, raw text data ($T_e = 4096$ text tokens) is rendered onto $M = 28$ images, resulting in $64 \times 28 = 1792$ visual tokens, passed to the cross-attention layer in LLM. This compression reduces the computational complexity of the cross-attention layer within the LLM. Moreover, the number of images M and tokens N can be dynamically adjusted during both training and inference, *allowing VIST to flexibly control the compression ratio*. VIST using a lightweight vision encoder, offers a more efficient approach than processing all text tokens directly within the LLM.

3.4 Probability-informed Visual Enhancement

In VIST, the frozen vision encoder is pre-trained primarily on general visual data (such as natural images) without exposure to rendered text images. Hence its ability to interpret dense textual information within images is constrained. To alleviate this problem, we develop a novel training objective, named Probability-informed Visual Enhancement (PVE). PVE enhances the understanding capabilities of Perceiver Resampler for rendered text images, enabling them to serve as robust substitutes for traditional text tokenizers.

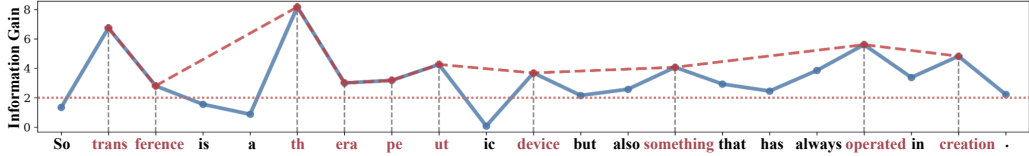


Figure 3: **Token-Level Information Gain (IG)** in sentence “*So transference is a therapeutic device but also something that has always operated in creation.*”. The red dashed line masks of 50% the most frequent tokens based on training set statistics. This strategy preserves tokens with higher information gain, while eliminating statistically prevalent but low-value tokens, enhancing semantic density.

Text-anchored Semantic Consistency. PVE encourages the Perceiver Resampler to learn a shared embedding space, aligning visual text features \mathbf{F}' with text token embeddings from text tokenizer. Concretely, PVE is formulated as a contrastive loss:

$$\mathcal{L}_{\text{PVE}}^{ij} = -\log \frac{\exp(\langle \hat{\mathbf{F}}_i', \hat{\mathbf{F}}_j^t \rangle / \tau)}{\sum_{k=1}^B \exp(\langle \hat{\mathbf{F}}_i', \hat{\mathbf{F}}_k^t \rangle / \tau)}, \quad (1)$$

where B is batch size and $\hat{\mathbf{F}}_i'$ is obtained by applying average pooling to the CLS tokens from \mathbf{F}_i' . $\hat{\mathbf{F}}_j^t$ is the averaged text token embedding after **frequency-based masking** and pooling. τ is the temperate parameter. Importantly, $\hat{\mathbf{F}}_i'$ and $\hat{\mathbf{F}}_j^t$ are different representations derived from the same text.

Frequency-based Masking. PVE employs text token embeddings as supervision signals to guide the Resampler in extracting textual information from text images. However, long-form text is inherently redundant, where structural components and function words may dominate the token distribution. Such redundancy introduces noise that impedes Resampler from capturing **key semantic content**.

Our solution draws inspiration from Shannon information theory [50], which provides a formal way to quantify the information content of an event or a message. The formula is given by:

$$I(y) = -\log_2 P(y), \quad (2)$$

where $I(y)$ is the information content of event or messages y and $P(y)$ is the probability of y . It highlights the inverse relationship between the probability of an event and the information it carries. When applied to tokens in a corpus: **Rare tokens** (low-frequency) are treated as high-information tokens because they often carry domain-specific or contextually important information. **Frequent tokens** (high-frequency) have lower information content because they may serve more structural or grammatical purposes, contributing less to the unique meaning of the text. Figure 3 shows that masking 50% of the most frequent tokens based on corpus-level (*i.e.*, training set) frequency distribution still *preserves most high-information-gain (IG) tokens, ensuring minimal loss of critical information while reducing redundancy*. This aligns with the **selective reading strategies** [10, 51] observed in skilled readers. Based on this principle, we devise frequency-based masking strategy that uses token frequency as a proxy for semantic importance. This strategy masks frequent tokens but low-information tokens to improve the information density of text token embeddings. The importance score for each token is calculated as follows:

$$s_w = \log \frac{|\mathcal{S}|}{1 + \text{count}(w)}, \quad (3)$$

where $|\mathcal{S}|$ denotes the total number of samples, $\text{count}(w)$ is the count of the token w (subword), and s_w is the importance score of token w . Token frequency statistics can be easily computed online with negligible overhead or precomputed. Based on the importance score for each token, we apply a 50% masking rate, where *tokens are randomly masked with tokens of lower importance score being more likely to be masked*. This ensures the Resampler prioritizes key content-bearing tokens, learning richer semantic representations and improving its ability to interpret dense text in rendered images.

4 Experiment

4.1 Experimental Setup

Pretraining. We validate ViST with TinyLlama [52]. The frozen vision encoder in our model is ViT-L/14 [11]. To reduce computational overhead, our model employs float16 precision and DeepSpeed Zero-2 with CPU off-loading [53].

Table 1: Text perplexity on the last 256 tokens of long-context language modeling for ArXiv and Book datasets, PG19, Proof, and Code. T_e is token length for encoder, and T_d is for LLM. \dagger denotes methods with the Resampler and PVE in our VIST. We report the Throughput of each model relative to TinyLlama. Δ is compression ratio.

| Method | T_e | T_d | ArXiv | Book | PG19 | Proof | Code | Throughput | Δ | TFLOPs | MEM(GB) |
|----------------------|--------|-------|--------------|---------------|---------------|--------------|--------------|----------------------|----------|------------------------------|------------------------------|
| TinyLlama [52] | - | 4096 | $> 10^3$ | $> 10^3$ | $> 10^3$ | $> 10^3$ | $> 10^3$ | 1.0 \times | - | 8.47 | 5.46 |
| Replug [54] | - | 4096 | 3.220 | 15.394 | 14.685 | 3.921 | 3.011 | 0.2 \times | - | 9.15 | 6.12 |
| Stream [55] | - | 4096 | 3.116 | 15.188 | 14.372 | 2.876 | 2.764 | 1.6 \times | - | 8.31 | 6.41 |
| ToMe \dagger [56] | 2048 | 2048 | 3.536 | 15.607 | 16.213 | 4.128 | 3.234 | 3.8 \times | 2.3 | 7.93 | 4.59 |
| FastV \dagger [57] | 2048 | 2048 | 3.491 | 15.711 | 16.016 | 4.216 | 3.111 | 3.8 \times | 2.3 | 7.88 | 4.59 |
| CEPE* [21] | 2048 | 2048 | 3.071 | 15.619 | 11.737 | 2.888 | 2.151 | 1.8 \times | - | 8.26 | 4.80 |
| VIST | 2048 | 2048 | 2.993 | 14.973 | 13.205 | 3.057 | 2.247 | 3.8 \times | 2.3 | 7.72(0.75\downarrow) | 4.59(0.87\downarrow) |
| CEPE* [21] | 6144 | 2048 | 3.005 | 14.919 | 11.112 | 2.719 | 2.100 | 2.1 \times | - | 13.27 | 7.74 |
| VIST | 6144 | 2048 | 2.989 | 14.894 | 12.737 | 3.003 | 2.183 | 5.3\mathtimes | 2.3 | 11.65(1.62\downarrow) | 4.94(2.80\downarrow) |
| CEPE* [21] | 14,336 | 2048 | 3.003 | 14.921 | 10.909 | 2.715 | 2.162 | 3.3 \times | - | 23.30 | 13.59 |
| VIST | 14,336 | 2048 | 2.965 | 14.815 | 11.933 | 2.971 | 2.032 | 7.6\mathtimes | 2.3 | 19.52(3.78\downarrow) | 6.75 (6.84\downarrow) |

Competitors. **i) Long-context models:** Replug [54] and Stream [55] with TinyLlama [52]. **ii) Text-encoder-based compression method:** To compare the effectiveness of leveraging text tokens v.s. visual tokens for processing long contexts in LLM, we implement CEPE* by applying CEPE [21] to TinyLlama [52], replacing the vision encoder in VIST with a lightweight text encoder. All other architectural and training settings are kept identical. **iii) Vision-centric compression methods:** ToMe [56] merges, and FastV [57] prunes visual features from frozen vision encoders. For fairness, we match their compression rates to ours. Directly using these visual features in LLMs leads to high perplexity ($>1k$) due to the mismatch between visual and text tokens. Thus, we retain the Resampler and PVE in our VIST, denoting ToMe \dagger and FastV \dagger .

Pretraining Dataset. Our pertaining dataset is an official sample of the RedPajama dataset [58], including 1B tokens from seven domains: ArXiv, Book, C4, Commoncrawl, GitHub, StackExchange, and Wikipedia. The training set of the corpus is preprocessed into 4608 text token sequences, where the first 4096 text token sequences are fed into the vision encoder (or text encoder for CEPE*) and the remaining 512 text tokens are provided to LLM.

Downstream Evaluation. We primarily evaluate tasks requiring long context processing, revealing vision tokens effectively handle extended context, outperforming previous text-encoder-based model.

4.2 Long-context Language Modeling

To assess the long-context language modeling (LCM) ability, we evaluate on ArXiv and Book from RedPajama [58] test split, alongside long-context datasets: PG19 [59], Proof [60], and Code [61]. The evaluation metric is perplexity (PPL) over the last 256 tokens of each input. Early tokens (typically farther from the current prediction point) are handled by the vision encoder, while the more recent tokens are passed to the LLM, under the assumption that proximity correlates with relevance.

Impact of Increased Text Length. Table 1 summarizes the results across different input lengths. Long-context language modeling can benefit from previous long contextual information. However, TinyLlama [52] supports only fixed-size inputs of 2048 tokens. Beyond this length, its performance drops sharply, with perplexity exceeding 10^3 . In contrast, VIST demonstrates a consistent decrease in perplexity as the input text length increases. Vision-centric token compression models ToMe \dagger and FastV \dagger focus on natural images, where redundancy arises from local visual similarity. However, they are *ill-suited for text redundancy and struggle to preserve key semantic content in text image*, yielding higher perplexity than our VIST. Moreover, VIST obtains the lowest PPL (14.973) on Book datasets, when T_e and T_d are 2048. These results prove that **VIST effectively enhances the capability of modeling long-form language.**

Comparison on Inference Cost. In Table 1, VIST renders text into multiple images of size 224×224 . 1024 text tokens need 7 images and VIST requires 56% fewer visual tokens than text tokens for the same input (*i.e.*, compression ratio Δ is 2.3, from 1024 text tokens to $448 = 7 \times 64$ visual tokens). We report the throughput of each model relative to TinyLlama. VIST achieves comparable performance with text-encoder-based compression model CEPE*, with 16% fewer FLOPs, 50% less memory usage, and higher throughput when processing 16k tokens.

Table 2: In-context learning accuracy averaged across 3 seeds (42, 43 and 44). Green highlights the gain from the additional demos. n_e is the number of demos for encoder and n_d for decoder (LLM).

| Method | n_e | n_d | SST2 | MR | AGN | SST5 | NLUS | NLUI | TREC | TREF | DBP | BANK | CLIN | Avg. |
|----------------|-------|-------|-------------|-------------|-------------|-------------|-------------|-------------|-------------|-------------|-------------|-------------|-------------|--------------------|
| TinyLlama [52] | - | 2 | 76.0 | 67.7 | 63.4 | 27.6 | 5.2 | 4.4 | 28.8 | 9.6 | 38.0 | 23.0 | 22.4 | 33.3 |
| TinyLlama [52] | - | 20 | 87.6 | 71.7 | 75.0 | 30.1 | 46.1 | 32.6 | 72.0 | 38.5 | 80.4 | 42.9 | 53.7 | 57.3(24.0↑) |
| CEPE* [21] | 18 | 2 | 76.9 | 82.3 | 66.9 | 29.1 | 9.6 | 30 | 39.2 | 12.7 | 71.1 | 27.2 | 39.8 | 44.1(10.8↑) |
| VIST | 18 | 2 | 77.7 | 79.2 | 61.5 | 42.7 | 15.6 | 40.6 | 36.5 | 14.6 | 71.9 | 25.0 | 43.8 | 46.3(13.0↑) |
| TinyLlama [52] | - | 50 | 88.6 | 64.8 | 21.4 | 42.5 | 34.2 | 30.4 | 81.1 | 44.7 | 3.4 | 49.7 | 39.7 | 45.5(12.2↑) |
| CEPE* [21] | 48 | 2 | 82.9 | 79.4 | 63.9 | 42.3 | 28.1 | 31.1 | 32.6 | 14.7 | 71.5 | 29.0 | 39.1 | 46.8(13.5↑) |
| VIST | 48 | 2 | 78.9 | 85.2 | 71.9 | 44.4 | 27.2 | 43.1 | 38.3 | 18.4 | 73.1 | 25.4 | 48.1 | 50.4(17.1↑) |

4.3 In-context Learning

We evaluate VIST on In-Context Learning (ICL) tasks across 11 widely-used text-classification datasets: SST2 [62], MR [63], AGN [64], SST5 [62], TREC, TREF [65], DBP [64], NLUS, NLUI [66], BANK [67], and CLIN [68]. Following [21], we randomly sample 250 text examples per dataset. The ICL results in Table 2 are reported as the average accuracy over three random seeds. For VIST and CEPE*, we provide two demonstrations directly to the decoder, while the rest are processed by the encoder.

Results. Table 2 examines the influence of increasing the number of demonstrations, where n_e is the number of demos for encoder and n_d for LLM. VIST shows a 13% accuracy improvement (from 33.3% to 46.3%) as more demonstrations (n_e is 18) are provided to the visual encoder, showcasing the capacity of LLM to comprehend text within visual signals when integrated with VIST. Furthermore, VIST outperforms CEPE* in average accuracy across all 11 datasets, which indicates **visual-based text understanding can effectively match or even surpass text encoder performance**. Though VIST and CEPE* ($n_e = 18, n_d = 2$) underperform TinyLlama ($n_d = 20$), they *achieve lower computational cost by processing most demonstrations (18) with lightweight encoder*. The performance gap on NLUS, TREC and TREF may stem from high category diversity, where the weak relevance between queries and demonstrations makes the lightweight encoding less effective than using the full LLM for all demos. Notably, the performance of TinyLlama declines with 50 demonstrations due to context window limit, while VIST remains efficient and stable.

4.4 Open-domain Question Answering

Open-domain Question Answering (QA) is a challenging task that requires model to generate accurate answers based on retrieved relevant information. Experiments are conducted on three open-domain QA datasets, including TriviaQA [69], NQ [70], and PopQA [71]. We use Contriever [72] to retrieve relevant k passages from Wikipedia, as in CEPE [21]. We prioritize passing the most relevant passages to the decoder to enhance performance. In Table 3, we report the exact match (EM) scores.

Results. TinyLlama is limited by a maximum context window of 2048 tokens, restricting it to processing no more than 10 passages at a time. Beyond this limit, performance drops sharply, with EM score falling below 1. For passages $k_d = 10$, the input already approaches or even exceeds the 2048-token limit of TinyLlama, so we truncate the input to avoid performance degradation. When processing 5 extra passages (*i.e.*, $k_e = 5, k_d = 10$), VIST results in an EM score improvement of **3.75** compared to TinyLlama on TriviaQA [69] dataset. Moreover, it even surpasses text encoder-based approach CEPE* under the same input conditions, *e.g.*, delivering an EM score **9.11** points higher on the TriviaQA dataset when $k_e = 20, k_d = 10$. *This enhancement may be attributed to PVE in VIST which leverages enriched text embeddings to guide the Resampler in capturing key semantics.* By emphasizing critical details and filtering out noise from lengthy inputs, our VIST prioritizes relevant information—a crucial factor for success in open-domain QA tasks. In contrast, CEPE* degrades when more passages are provided to the encoder,

Table 3: **Open-domain QA results.** k_e represents the number of passages provided to the encoder, while k_d denotes the number of passages given to the LLM. We report the exact match score.

| Method | k_e | k_d | TriviaQA | NQ | PopQA |
|----------------|-------|-------|---------------------|--------------------|---------------------|
| TinyLlama [52] | - | 10 | 21.45 | 8.45 | 10.79 |
| TinyLlama [52] | - | 15 | < 1 | < 1 | < 1 |
| VIST | 10 | 0 | 21.27 | 8.51 | 10.67 |
| CEPE* [21] | 5 | 10 | 16.41 | 6.09 | 4.92 |
| VIST | 5 | 10 | 25.20(8.79↑) | 8.71(2.62↑) | 11.44(6.52↑) |
| CEPE* [21] | 20 | 10 | 16.56 | 6.75 | 5.78 |
| VIST | 20 | 10 | 25.67(9.11↑) | 8.81(2.06↑) | 11.84(6.06↑) |

Table 4: The effect of visual token count for each image.

| Tokens Per Image | ICL | | Open-domain QA | | |
|---------------------|-------------|-------------|----------------|-------------|--------------|
| | TREC | MR | TriviaQA | NQ | PopQA |
| 32 | 32.7 | 78.8 | 19.38 | 7.85 | 8.16 |
| 64 | 36.5 | 79.2 | 25.20 | 8.71 | 11.44 |
| 96 | 32.0 | 79.7 | 14.57 | 7.19 | 4.88 |
| 128 | 32.9 | 87.0 | 20.01 | 7.77 | 8.51 |

Table 5: The effect of different masking strategies in PVE. FM is frequency-based masking strategy, RM is random masking. The masking ratio is set to 50%.

| RM | FM | ICL | | Open-domain QA | | |
|----|----|-------------|-------------|----------------|-------------|--------------|
| | | NLUS | NLUI | TriviaQA | NQ | PopQA |
| | | 9.9 | 26.4 | 17.14 | 6.51 | 5.72 |
| ✓ | | 8.3 | 30.2 | 24.88 | 8.35 | 10.19 |
| ✓ | ✓ | 15.6 | 40.6 | 25.20 | 8.71 | 11.44 |

Table 6: Ablation on the length of text inputs (in tokens).

| Encoder | ICL | | Open-domain QA | | |
|---------|--------------|-------------|----------------|-------------|--------------|
| | Input Length | SST5 | MR | TriviaQA | NQ |
| 1024 | 39.6 | 85.9 | 19.77 | 6.47 | 6.63 |
| 2048 | 39.3 | 73.8 | 22.85 | 8.08 | 9.77 |
| 4096 | 42.7 | 79.2 | 25.20 | 8.71 | 11.44 |
| 6144 | 37.8 | 90.5 | 27.52 | 9.24 | 13.49 |

Table 7: VIST effectively reduces PPL on LCM and improves accuracy on ICL by processing additional context. \dagger means our implementation on Mistral 7B [73].

| Method | LCM | | ICL | |
|----------------|--|---|---------------------------------------|---------------------------------------|
| | Arxiv | Book | SST2 | DBP |
| Mistral | 2.93 | 12.82 | 89.1 | 93.6 |
| CEPE \dagger | 2.83(0.10 \downarrow) | 12.64(0.18 \downarrow) | 90.8(1.7 \uparrow) | 94.2(0.6 \uparrow) |
| VIST \dagger | 2.82(0.11\downarrow) | 12.61(0.21\downarrow) | 92.8(3.7\uparrow) | 95.3(1.7\uparrow) |

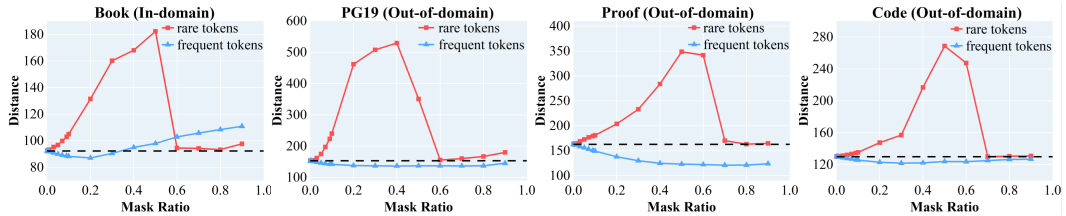


Figure 4: Effect of frequent vs. rare tokens on semantic integrity. Masking rare tokens (red) significantly disrupts semantic representation, increasing text-visual embedding distance, while masking frequent tokens (blue) has minimal impact, demonstrating that rare tokens are critical for preserving semantic meaning.

as additional passages introduce more noise and redundancy, making it harder to extract relevant answers. We also investigate the effectiveness of using only the fast path of VIST (*i.e.*, vision encoder) on the Open-domain QA task, which requires the model to generate accurate answers based on given relevant passages. Specifically, we feed only the top-10 relevant passages to the visual encoder (*i.e.*, $k_e = 10$), without providing any passages to the LLM directly (*i.e.*, setting $k_d = 0$). Surprisingly, this configuration yields performance on par with TinyLLaMA, despite the latter processing all 10 passages with a much heavier LLM. This demonstrates that the fast path of our method can distill and preserve the critical information from long contexts, providing a compact yet effective representation.

4.5 Ablation Study

We explore the effects of ① the masking strategy employed in PVE, ② the length of text provided to the encoder during training, ③ the number of compressed tokens in each image (*i.e.*, N in §3.3), and ④ extension to other LLM. In open-domain QA tasks, the model is fed 10 passages for LLM and 5 for encoder. ICL tasks use a fixed setup of 18 demonstrations for encoder and 2 for LLM.

Number of Tokens in Each Image. The Resampler transforms image features into a fixed number of visual tokens. Table 4 analyzes the impact of visual token count for each image. Increasing the number of visual tokens reduces compression ratio, but as shown, **a lower compression ratio does not always yield better results**. With 64 visual tokens, the model performs best on 4 out of 5 datasets, whereas 128 tokens only perform best on MR dataset. This discrepancy could be attributed to the trade-off between the amount of information preserved and the noise introduced during compression. Fewer tokens risk losing critical details, while more tokens may retain irrelevant information, which can hinder generalization. These findings emphasize that achieving a balance between compression and information retention is crucial for optimal performance across different datasets.

Masking Strategy in PVE (§3.4). Long texts often contain significant redundancy. To address this, we integrate a Frequency-based Masking (FM) strategy into PVE, improving the information density of text token embeddings. Table 5 compares the performance of VIST with FM, w/o FM, and with random masking. Excluding FM causes a notable decline in ICL and open-domain QA performance. This highlights the critical role of information-dense text token embeddings in guiding the visual encoder to capture more semantically meaningful and discriminative features.

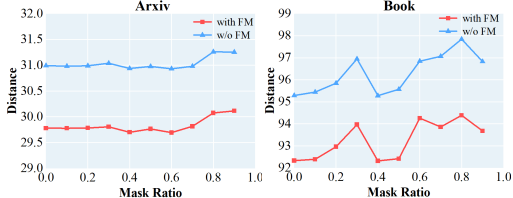


Figure 5: Impact of Frequency-based Masking on Text-Visual Semantic Distance. Compared to model without FM, VIST with FM consistently reduces the semantic distance between text token embeddings and visual features, across all masking ratios.

In-context Text Length. Table 6 investigates the impact of in-context text length (measured in text tokens) provided to the visual encoder during training. Our model, trained with a longer encoder input length, generally yields higher EM scores on open-domain QA tasks. This may be because exposure to more lengthy texts during training helps our model better extract key information from extensive contexts, which is crucial for open-domain QA. Table 6 shows that longer training text inputs often boost ICL task accuracy. For instance, the best result on SST5 (42.7) was achieved with an encoder input length of 4096 text tokens, while the highest accuracy on MR (90.5) was obtained with the longest input length of 6144 tokens. Interestingly, we observed that training with an input length of 1024 tokens performed comparably to 2048 tokens, possibly because the total demo length for the encoder was close to 1024 tokens.

Extension to Other LLM. Mixture-of-expert models effectively scale model capacity while saving resources. To prove the generality of VIST, we also apply VIST to Mistral 7B [73]. In LCM task, VIST[‡] and CEPE[‡] process 4096 tokens, compared to the 2048 tokens processed by Mistral. For ICL, VIST[‡] and CEPE[‡] use 20 demonstrations, while Mistral uses only 2. As shown in Table 7, VIST[‡] demonstrates superior performance over CEPE[‡], by effectively leveraging additional context.

5 Discussion

Exploring Token Frequency as a Proxy for Semantic Importance. To assess the impact of rare versus frequent text tokens on global semantics across in-domain (Book [58]) and out-of-domain datasets (PG19 [59], Proof [60], and Code [61]), we first calculate importance score for each token using Eq. 3 based on training-set token frequency statistics. Two masking operations are then applied to the text token embeddings: ① Masking tokens with high importance scores (red line in Figure 4). ② Masking tokens with low importance scores (blue line in Figure 4). The distance between masked text embeddings and visual features is computed.

At low masking ratios (0.0 to 0.4), masking rare tokens causes a sharp increase in distance, while masking frequent tokens has minimal impact and even reduces distance. This suggests that rare tokens carry more critical semantic information, and their removal disrupts the alignment between text and visual tokens. In contrast, frequent tokens may contain more redundant or less informative content, so masking them has little impact or even improves the alignment by reducing noise. These findings support the hypothesis that *token frequency is a reasonable indicator of semantic importance, with rare tokens playing a more pivotal role in preserving semantic integrity*.

The Effect of Frequency-based Masking on Text-Visual Semantic Gap. VIST employs Frequency-based Masking (FM) within the Probability-informed Visual Enhancement to improve the semantic richness of text token embeddings. Figure 5 presents the impact of FM on the semantic alignment between text token embeddings and visual features extracted by the Perceiver Resampler. We experimented with random masking ratios (0.0 to 0.9) on text token embeddings and calculated the sum of cosine distances across all test samples in the Arxiv and Book datasets [58]. Across all ratios, VIST with FM consistently exhibits smaller semantic distances than VIST without FM, highlighting FM effectively enhances semantic coherence.

Token Redundancy Visualization. We study the semantic contribution of frequent tokens by selectively masking the top 50% most frequent tokens (based on training set statistics). Figure 6 illustrates key nouns are fully preserved. The masked tokens mainly include function words (e.g., “the”, “of”), primarily serving grammatical roles rather than conveying core semantic meaning. This

The “primary identification” with the “father in individual prehistory” would be the means, the link that might enable one to become reconciled with the loss of the Thing. Primary identification initiates a compensation for the Thing and at the same time secures the subject to another dimension, that of **imaginary adherence**, reminding one of the bond of faith, which is just what disintegrates in the depressed person.

Figure 6: Visualization of Masking Frequent Tokens. Though we mask the top 50% most frequent tokens (based on training statistics), **key nouns** are completely preserved, proving that frequent tokens contribute less to semantic meaning.

proves FM strategy can **preserve critical semantic information while filtering out less relevant noise, thereby enhancing the ability of the model to focus on meaningful content.**

6 Conclusion

In-context learning with longer input sequences remains a prominent yet challenging topic in large language models (LLMs). In this work, we introduce a fully novel perspective to address this challenge by leveraging much lightweight visual encoder. To support longer input sequences in LLMs, we present VIST, a vision-centric token expansion method built upon a visual encoder framework. Our analysis further reveals there exists significant redundancy in text tokens, further validating the effectiveness and efficiency of our vision-encoder-based approach. With these advancements, VIST surpasses text-encoder-based token compression counterparts in both performance and efficiency. In future work, we plan to evaluate VIST across a broader range of downstream tasks and conduct a deeper investigation into text token redundancy.

References

- [1] Tom Brown, Benjamin Mann, Nick Ryder, Melanie Subbiah, Jared D Kaplan, Prafulla Dhariwal, Arvind Neelakantan, Pranav Shyam, Girish Sastry, Amanda Askell, et al. Language models are few-shot learners. In *Advances in neural information processing systems*, volume 33, pages 1877–1901, 2020.
- [2] Jinze Bai, Shuai Bai, Yunfei Chu, Zeyu Cui, Kai Dang, Xiaodong Deng, Yang Fan, Wenbin Ge, Yu Han, Fei Huang, Binyuan Hui, Luo Ji, Mei Li, Junyang Lin, Runji Lin, Dayiheng Liu, Gao Liu, Chengqiang Lu, Keming Lu, Jianxin Ma, Rui Men, Xingzhang Ren, Xuancheng Ren, Chuanqi Tan, Sinan Tan, Jianhong Tu, Peng Wang, Shijie Wang, Wei Wang, Shengguang Wu, Benfeng Xu, Jin Xu, An Yang, Hao Yang, Jian Yang, Shusheng Yang, Yang Yao, Bowen Yu, Hongyi Yuan, Zheng Yuan, Jianwei Zhang, Xingxuan Zhang, Yichang Zhang, Zhenru Zhang, Chang Zhou, Jingren Zhou, Xiaohuan Zhou, and Tianhang Zhu. Qwen technical report. *arXiv preprint arXiv:2309.16609*, 2023.
- [3] Saku Sugawara, Xanh Ho, Anh-Khoa Duong Nguyen, and Akiko Aizawa. Constructing a multi-hop qa dataset for comprehensive evaluation of reasoning steps. In *Proceedings of the 28th International Conference on Computational Linguistics*. International Committee on Computational Linguistics, 2020.
- [4] Harsh Trivedi, Niranjan Balasubramanian, Tushar Khot, and Ashish Sabharwal. musique: Multihop questions via single-hop question composition. *Transactions of the Association for Computational Linguistics*, 10:539–554, 2022.
- [5] Josh Achiam, Steven Adler, Sandhini Agarwal, Lama Ahmad, Ilge Akkaya, Florencia Leoni Aleman, Diogo Almeida, Janko Altenschmidt, Sam Altman, Shyamal Anadkat, et al. Gpt-4 technical report. *arXiv preprint arXiv:2303.08774*, 2023.
- [6] Yichun Yin, Wenyong Huang, Kaikai Song, Yehui Tang, Xueyu Wu, Wei Guo, Peng Guo, Yaoyuan Wang, Xiaojun Meng, Yasheng Wang, et al. Pangu ultra: Pushing the limits of dense large language models on ascend npus. *arXiv preprint arXiv:2504.07866*, 2025.
- [7] Xiang Li, Yiqun Yao, Xin Jiang, Xuezhi Fang, Chao Wang, Xinzheng Liu, Zihan Wang, Yu Zhao, Xin Wang, Yuyao Huang, et al. 52b to 1t: Lessons learned via tele-flm series. *arXiv preprint arXiv:2407.02783*, 2024.
- [8] Keith Rayner, Erik D Reichle, Michael J Stroud, Carrick C Williams, and Alexander Pollatsek. The effect of word frequency, word predictability, and font difficulty on the eye movements of young and older readers. *Psychology and aging*, 21(3):448, 2006.
- [9] Alexander Strukelj and Diederick C Niehorster. One page of text: Eye movements during regular and thorough reading, skimming, and spell checking. *Journal of Eye Movement Research*, 11(1):10–16910, 2018.
- [10] Ziwei Gu, Owen Raymond, Naser Al Madi, and Elena L Glassman. Why do skimmers perform better with grammar-preserving text saliency modulation (gp-tsm)? evidence from an eye tracking study. In *Extended Abstracts of the CHI Conference on Human Factors in Computing Systems*, pages 1–8, 2024.
- [11] Alec Radford, Jong Wook Kim, Chris Hallacy, Aditya Ramesh, Gabriel Goh, Sandhini Agarwal, Girish Sastry, Amanda Askell, Pamela Mishkin, Jack Clark, et al. Learning transferable visual models from natural language supervision. In *International Conference on Machine Learning*, pages 8748–8763, 2021.

[12] Yiqi Lin, Conghui He, Alex Jinpeng Wang, Bin Wang, Weijia Li, and Mike Zheng Shou. Parrot captions teach clip to spot text. In *European Conference on Computer Vision*, pages 368–385. Springer, 2025.

[13] Yucheng Li, Bo Dong, Frank Guerin, and Chenghua Lin. Compressing context to enhance inference efficiency of large language models. In *Proceedings of the 2023 Conference on Empirical Methods in Natural Language Processing*, pages 6342–6353, 2023.

[14] Huiqiang Jiang, Qianhui Wu, Chin-Yew Lin, Yuqing Yang, and Lili Qiu. Llmlingua: Compressing prompts for accelerated inference of large language models. In *Proceedings of the 2023 Conference on Empirical Methods in Natural Language Processing*, pages 13358–13376, 2023.

[15] Kolby Nottingham, Yasaman Razeghi, Kyungmin Kim, JB Lanier, Pierre Baldi, Roy Fox, and Sameer Singh. Selective perception: Learning concise state descriptions for language model actors. In *Association for Computational Linguistics*, pages 327–341, 2024.

[16] Huiqiang Jiang, Qianhui Wu, Xufang Luo, Dongsheng Li, Chin-Yew Lin, Yuqing Yang, and Lili Qiu. Longllmlingua: Accelerating and enhancing llms in long context scenarios via prompt compression. *arXiv preprint arXiv:2310.06839*, 2023.

[17] Zhuoshi Pan, Qianhui Wu, Huiqiang Jiang, Menglin Xia, Xufang Luo, Jue Zhang, Qingwei Lin, Victor Rühle, Yuqing Yang, Chin-Yew Lin, et al. Llmlingua-2: Data distillation for efficient and faithful task-agnostic prompt compression. *arXiv preprint arXiv:2403.12968*, 2024.

[18] Philip Gage. A new algorithm for data compression. *The C Users Journal*, 12(2):23–38, 1994.

[19] Yintao Tai, Xiyang Liao, Alessandro Suglia, and Antonio Vergari. Pixar: Auto-regressive language modeling in pixel space. *arXiv preprint arXiv:2401.03321*, 2024.

[20] Phillip Rust, Jonas F Lotz, Emanuele Bugliarello, Elizabeth Salesky, Miryam de Lhoneux, and Desmond Elliott. Language modelling with pixels. In *International Conference on Learning Representations*, 2022.

[21] Howard Yen, Tianyu Gao, and Danqi Chen. Long-context language modeling with parallel context encoding. In *Association for Computational Linguistics*, 2024.

[22] David Wingate, Mohammad Shoeybi, and Taylor Sorensen. Prompt compression and contrastive conditioning for controllability and toxicity reduction in language models. In *Findings of the Association for Computational Linguistics: EMNLP 2022*, pages 5621–5634, 2022.

[23] Peitian Zhang, Zheng Liu, Shitao Xiao, Ninglu Shao, Qiwei Ye, and Zhicheng Dou. Soaring from 4k to 400k: Extending llm’s context with activation beacon. *arXiv preprint arXiv:2401.03462*, 2024.

[24] Jesse Mu, Xiang Li, and Noah Goodman. Learning to compress prompts with gist tokens. In *Advances in Neural Information Processing Systems*, volume 36, 2024.

[25] Alexis Chevalier, Alexander Wettig, Anirudh Ajith, and Danqi Chen. Adapting language models to compress contexts. In *Proceedings of the 2023 Conference on Empirical Methods in Natural Language Processing*, pages 3829–3846, 2023.

[26] Tao Ge, Hu Jing, Lei Wang, Xun Wang, Si-Qing Chen, and Furu Wei. In-context autoencoder for context compression in a large language model. In *International Conference on Learning Representations*, 2024.

[27] Yuhong Li, Yingbing Huang, Bowen Yang, Bharat Venkitesh, Acyr Locatelli, Hanchen Ye, Tianle Cai, Patrick Lewis, and Deming Chen. Snapkv: Llm knows what you are looking for before generation. In *Advances in Neural Information Processing Systems*, volume 37, pages 22947–22970, 2024.

[28] Amirkeivan Mohtashami and Martin Jaggi. Random-access infinite context length for transformers. In *Advances in Neural Information Processing Systems*, volume 36, pages 54567–54585, 2023.

[29] Szymon Tworkowski, Konrad Staniszewski, Mikołaj Pącek, Yuhuai Wu, Henryk Michalewski, and Piotr Miłoś. Focused transformer: Contrastive training for context scaling. In *Advances in Neural Information Processing Systems*, volume 36, 2024.

[30] Peng Xu, Wei Ping, Xianchao Wu, Lawrence McAfee, Chen Zhu, Zihan Liu, Sandeep Subramanian, Evelina Bakhturina, Mohammad Shoeybi, and Bryan Catanzaro. Retrieval meets long context large language models. In *The Twelfth International Conference on Learning Representations*.

[31] Peitian Zhang, Shitao Xiao, Zheng Liu, Zhicheng Dou, and Jian-Yun Nie. Retrieve anything to augment large language models. *arXiv preprint arXiv:2310.07554*, 2023.

[32] Yuhuai Wu, Markus Norman Rabe, DeLesley Hutchins, and Christian Szegedy. Memorizing transformers. In *International Conference on Learning Representations*.

[33] Weizhi Wang, Li Dong, Hao Cheng, Xiaodong Liu, Xifeng Yan, Jianfeng Gao, and Furu Wei. Augmenting language models with long-term memory. In *Advances in Neural Information Processing Systems*, volume 36, 2024.

[34] Jacob Devlin Ming-Wei Chang Kenton and Lee Kristina Toutanova. Bert: Pre-training of deep bidirectional transformers for language understanding. In *Proceedings of NAACL-HLT*, volume 1, page 2, 2019.

[35] Taku Kudo and John Richardson. SentencePiece: A simple and language independent subword tokenizer and detokenizer for neural text processing. In *Proceedings of the 2018 Conference on Empirical Methods in Natural Language Processing*, pages 66–71, 2018.

[36] Rico Sennrich, Barry Haddow, and Alexandra Birch. Neural machine translation of rare words with subword units. In *Association for Computational Linguistics*, pages 1715–1725, 2016.

[37] Elizabeth Salesky, David Etter, and Matt Post. Robust open-vocabulary translation from visual text representations. In *Proceedings of the 2021 Conference on Empirical Methods in Natural Language Processing*, 2021.

[38] Tianyu Gao, Zirui Wang, Adithya Bhaskar, and Danqi Chen. Improving language understanding from screenshots. *arXiv preprint arXiv:2402.14073*, 2024.

[39] Yekun Chai, Qingyi Liu, Jingwu Xiao, Shuohuan Wang, Yu Sun, and Hua Wu. Dual modalities of text: Visual and textual generative pre-training. *arXiv preprint arXiv:2404.10710*, 2024.

[40] Jonas Lotz, Elizabeth Salesky, Phillip Rust, and Desmond Elliott. Text rendering strategies for pixel language models. In *Proceedings of the 2023 Conference on Empirical Methods in Natural Language Processing*, pages 10155–10172, 2023.

[41] Chenghao Xiao, Zhuoxu Huang, Danlu Chen, G Thomas Hudson, Yizhi Li, Haoran Duan, Chenghua Lin, Jie Fu, Jungong Han, and Noura Al Moubayed. Pixel sentence representation learning. *arXiv preprint arXiv:2402.08183*, 2024.

[42] Geewook Kim, Teakgyu Hong, Moonbin Yim, JeongYeon Nam, Jinyoung Park, Jinyeong Yim, Wonseok Hwang, Sangdoo Yun, Dongyoon Han, and Seunghyun Park. Ocr-free document understanding transformer. In *European Conference on Computer Vision*, pages 498–517, 2022.

[43] Kenton Lee, Mandar Joshi, Iulia Raluca Turc, Hexiang Hu, Fangyu Liu, Julian Martin Eisenschlos, Urvashi Khandelwal, Peter Shaw, Ming-Wei Chang, and Kristina Toutanova. Pix2struct: Screenshot parsing as pretraining for visual language understanding. In *International Conference on Machine Learning*, pages 18893–18912, 2023.

[44] Michael Tschannen, Basil Mustafa, and Neil Houlsby. Clippo: Image-and-language understanding from pixels only. In *Proceedings of the IEEE/CVF Conference on Computer Vision and Pattern Recognition*, pages 11006–11017, 2023.

[45] Alex Jinpeng Wang, Linjie Li, Yiqi Lin, Min Li, Lijuan Wang, and Mike Zheng Shou. Leveraging visual tokens for extended text contexts in multi-modal learning. In *Advances in Neural Information Processing Systems*, 2024.

[46] Xiujun Li, Yujie Lu, Zhe Gan, Jianfeng Gao, William Yang Wang, and Yejin Choi. Text as images: Can multimodal large language models follow printed instructions in pixels? *arXiv preprint arXiv:2311.17647*, 2023.

[47] Liang Zhang, Anwen Hu, Jing Zhang, Shuo Hu, and Qin Jin. Mpmqa: multimodal question answering on product manuals. In *Proceedings of the AAAI Conference on Artificial Intelligence*, volume 37, pages 13958–13966, 2023.

[48] Anwen Hu, Haiyang Xu, Liang Zhang, Jiabo Ye, Ming Yan, Ji Zhang, Qin Jin, Fei Huang, and Jingren Zhou. mplug-docowl2: High-resolution compressing for ocr-free multi-page document understanding. *arXiv preprint arXiv:2409.03420*, 2024.

[49] Jean-Baptiste Alayrac, Jeff Donahue, Pauline Luc, Antoine Miech, Iain Barr, Yana Hasson, Karel Lenc, Arthur Mensch, Katherine Millican, Malcolm Reynolds, et al. Flamingo: a visual language model for few-shot learning. In *Advances in neural information processing systems*, volume 35, pages 23716–23736, 2022.

[50] Claude Elwood Shannon. A mathematical theory of communication. *The Bell system technical journal*, 27(3):379–423, 1948.

[51] Marc Brysbaert and Françoise Vitu. Word skipping: Implications for theories of eye movement control in reading. In *Eye guidance in reading and scene perception*, pages 125–147. Elsevier, 1998.

[52] Peiyuan Zhang, Guangtao Zeng, Tianduo Wang, and Wei Lu. Tinyllama: An open-source small language model. *arXiv preprint arXiv:2401.02385*, 2024.

[53] Jeff Rasley, Samyam Rajbhandari, Olatunji Ruwase, and Yuxiong He. Deepspeed: System optimizations enable training deep learning models with over 100 billion parameters. In *Proceedings of the 26th ACM SIGKDD International Conference on Knowledge Discovery & Data Mining*, pages 3505–3506, 2020.

[54] Weijia Shi, Sewon Min, Michihiro Yasunaga, Minjoon Seo, Rich James, Mike Lewis, Luke Zettlemoyer, and Wen Tau Yih. Replug: Retrieval-augmented black-box language models. In *2024 Conference of the North American Chapter of the Association for Computational Linguistics: Human Language Technologies, NAACL 2024*, pages 8364–8377, 2024.

[55] Guangxuan Xiao, Yuandong Tian, Beidi Chen, Song Han, and Mike Lewis. Efficient streaming language models with attention sinks. In *The Twelfth International Conference on Learning Representations*.

[56] Daniel Bolya, Cheng-Yang Fu, Xiaoliang Dai, Peizhao Zhang, Christoph Feichtenhofer, and Judy Hoffman. Token merging: Your vit but faster. In *International Conference on Learning Representations*.

[57] Liang Chen, Haozhe Zhao, Tianyu Liu, Shuai Bai, Junyang Lin, Chang Zhou, and Baobao Chang. An image is worth 1/2 tokens after layer 2: Plug-and-play inference acceleration for large vision-language models. In *European Conference on Computer Vision*, pages 19–35. Springer, 2024.

[58] Maurice Weber, Daniel Y. Fu, Quentin Anthony, Yonatan Oren, Shane Adams, Anton Alexandrov, Xiaozhong Lyu, Huu Nguyen, Xiaozhe Yao, Virginia Adams, Ben Athiwaratkun, Rahul Chalamala, Kezhen Chen, Max Ryabinin, Tri Dao, Percy Liang, Christopher Ré, Irina Rish, and Ce Zhang. Redpajama: an open dataset for training large language models. In *Advances in Neural Information Processing Systems*, 2024.

[59] Jack W Rae, Anna Potapenko, Siddhant M Jayakumar, Chloe Hillier, and Timothy P Lillicrap. Compressive transformers for long-range sequence modelling. In *International Conference on Learning Representations*, 2019.

[60] Zhangir Azerbayev, Edward Ayers, and Bartosz Piotrowski. Proofpile: A pre-training dataset of mathematical texts. 2023.

[61] Thomas Wolf, Loubna Ben Allal, Leandro von Werra, Li Jia, and Armel Zebaze. A dataset of python files from github, 2023.

[62] Richard Socher, Alex Perelygin, Jean Wu, Jason Chuang, Christopher D Manning, Andrew Y Ng, and Christopher Potts. Recursive deep models for semantic compositionality over a sentiment treebank. In *Proceedings of the 2013 conference on empirical methods in natural language processing*, pages 1631–1642, 2013.

[63] Bo Pang and Lillian Lee. Seeing stars: Exploiting class relationships for sentiment categorization with respect to rating scales. In *Association for Computational Linguistics*, pages 115–124, 2005.

[64] Xiang Zhang, Junbo Zhao, and Yann LeCun. Character-level convolutional networks for text classification. In *Advances in neural information processing systems*, volume 28, 2015.

[65] Ellen M Voorhees and Dawn M Tice. Building a question answering test collection. In *Proceedings of the 23rd annual international ACM SIGIR conference on Research and development in information retrieval*, pages 200–207, 2000.

[66] Xingkun Liu, Arash Eshghi, Paweł Swietojanski, and Verena Rieser. Benchmarking natural language understanding services for building conversational agents. In *Increasing naturalness and flexibility in spoken dialogue interaction: 10th international workshop on spoken dialogue systems*, pages 165–183. Springer, 2021.

[67] Iñigo Casanueva, Tadas Temčinas, Daniela Gerz, Matthew Henderson, and Ivan Vulić. Efficient intent detection with dual sentence encoders. In *Proceedings of the 2nd Workshop on Natural Language Processing for Conversational AI*, pages 38–45, 2020.

- [68] Stefan Larson, Anish Mahendran, Joseph J Peper, Christopher Clarke, Andrew Lee, Parker Hill, Jonathan K Kummerfeld, Kevin Leach, Michael A Laurenzano, Lingjia Tang, et al. An evaluation dataset for intent classification and out-of-scope prediction. In *Proceedings of the 2019 Conference on Empirical Methods in Natural Language Processing*, pages 1311–1316, 2019.
- [69] Mandar Joshi, Eunsol Choi, Daniel S Weld, and Luke Zettlemoyer. Triviaqa: A large scale distantly supervised challenge dataset for reading comprehension. In *Association for Computational Linguistics*, pages 1601–1611, 2017.
- [70] Tom Kwiatkowski, Jennimaria Palomaki, Olivia Redfield, Michael Collins, Ankur Parikh, Chris Alberti, Danielle Epstein, Illia Polosukhin, Jacob Devlin, Kenton Lee, et al. Natural questions: a benchmark for question answering research. *Transactions of the Association for Computational Linguistics*, 7:453–466, 2019.
- [71] Alex Mallen, Akari Asai, Victor Zhong, Rajarshi Das, Daniel Khashabi, and Hannaneh Hajishirzi. When not to trust language models: Investigating effectiveness of parametric and non-parametric memories. In *Association for Computational Linguistics*, pages 9802–9822, 2023.
- [72] Gautier Izacard, Mathilde Caron, Lucas Hosseini, Sebastian Riedel, Piotr Bojanowski, Armand Joulin, and Edouard Grave. Unsupervised dense information retrieval with contrastive learning. *Transactions on Machine Learning Research*, 2022.
- [73] Albert Q Jiang, Alexandre Sablayrolles, Arthur Mensch, Chris Bamford, Devendra Singh Chaplot, Diego de las Casas, Florian Bressand, Gianna Lengyel, Guillaume Lample, Lucile Saulnier, et al. Mistral 7b. *arXiv preprint arXiv:2310.06825*, 2023.